

Using $1/f$ noise to examine planning and control in a discrete aiming task

André B. Valdez · Eric L. Amazeen

Received: 19 September 2007 / Accepted: 2 February 2008 / Published online: 19 February 2008
© Springer-Verlag 2008

Abstract The present study used $1/f$ noise to examine how spatial, physical, and timing constraints affect planning and control processes in aiming. Participants moved objects of different masses to different distances at preferred speed (Experiment 1) and as quickly as possible (Experiment 2). Power spectral density, standardized dispersion, rescaled range, and an autoregressive fractionally integrated moving average (ARFIMA) model selection procedure were used to quantify $1/f$ noise. Measures from all four analyses were in reasonable agreement, with more ARFIMA (long-range) models selected at peak velocity in Experiment 1 and fewer selected at peak velocity in Experiment 2. There also was a nonsignificant trend where, at preferred speed, of those participants who showed $1/f$ noise, more tended to show $1/f$ noise at peak velocity, when planning and control would overlap most. This trend disappeared for fast movements, where planning and control would have less time to overlap. Summing short-range processes at different timescales can produce $1/f$ -like noise. As planning is a slower-moving process and control faster, present results suggest that, with enough time for both planning and control, $1/f$ noise in aiming may arise from a similar summation of processes. Potential limitations of time series length in the present task are discussed.

Keywords $1/f$ Noise · Long-range correlation · Fractal · Planning · Control

Introduction

There is recent evidence of long-range correlation, or $1/f$ noise, in discrete aiming (Miyazaki et al. 2001) and that this correlation occurs primarily during the initial stage of the movement. $1/f$ noise (defined in more detail below) indicates that variability at one point in time is positively correlated with variability at a later point, suggesting that behavior on early trials affects future behavior. According to Miyazaki et al. (2001), $1/f$ noise at the start of the movement may reflect the use of adjustment processes for initial variability, where such adjustment serves to reduce later error at the target (e.g., Gordon and Ghez 1987; Messier and Kalaska 1999). In the evidence cited, however, there was only one target distance, constant mass, and participants had to move as quickly as possible. This does not take into account the spatial, physical, and timing constraints in most common situations. With such constraints, it may be that the pattern and intensity of $1/f$ noise changes throughout the movement, implying that $1/f$ noise is perhaps context dependent and reflects the use of more than one process (e.g., planning and control). To further examine $1/f$ noise, movement constraints, and planning and control processes, the present study manipulated target distance, mass, and timing constraints in a discrete aiming task.

Planning and control

Woodworth (1899) was the first to suggest that aiming is comprised of an initial impulse phase and an ongoing control phase, where the initial impulse brings the limb into target range, and control adjusts movement trajectory based on visual feedback to reach the target (see Elliott et al. 2001 for an overview; and Keele 1968 for review of processing-based theory that built on Woodworth's model). Thus, the

A. B. Valdez (✉) · E. L. Amazeen
Department of Psychology,
Arizona State University, Box 871104, Tempe,
AZ 85287, USA
e-mail: andre.valdez@asu.edu

planning stage of movement may be conceptualized as an open-loop system; and the control stage, a closed-loop system (Schmidt and Lee 2005). A plan patterns movement instructions in advance and is not sensitive to environmental feedback, and control regulates movement online based on the input of movement-produced feedback (i.e., sensory information). It is assumed that planning is totally responsible for determining initial movement parameters, while control exerts greater influence as the movement unfolds, and that both stages overlap through time (see Desmurget and Grafton 2000; Wolpert and Ghahramani 2000; Wolpert et al. 1995).

The respective influence of planning and control also depends on factors such as timing, availability of feedback, and predictability. For instance, while control depends heavily on feedback loops (i.e., visual and proprioceptive) and will have greater influence when these loops have more time to operate, planning is more influential during movements of short duration (Glover 2004), as rapid actions (whose timeframe is less than about 150 ms) do not allow enough time to generate and detect an error signal, determine and initiate a correction, or complete the correction before the movement's end (Schmidt and Lee 2005). Uncertainty about the availability of feedback, on the other hand, may lead participants to adopt a more plan-based mode of limb control, where participants might be preparing for a 'worst-case scenario' where no feedback would be available (Hansen et al. 2006). And perhaps not surprisingly, the more predictable the movement, the more it will draw upon planning; the less so, the more planning will cede its influence to control (Glover 2004). Glover (2004) gave the example of running over uneven terrain, where the unpredictable contour would not allow for sustained planning but rather the increasing engagement of control processes.

1/f Noise: a new perspective

In a given movement, then, the crossover between planning and control would involve variability, and variability often is treated as error, both theoretically and statistically. However, patterns of serial correlation in variability may reveal more sophisticated and organized phenomena (e.g., see Ding et al. 2002; Farrell et al. 2006; Thornton and Gildea 2005; van Orden et al. 2003; Wagenmakers et al. 2004). For example, at a neural level, different movement tasks (synchronized vs. syncopated tapping) showing a different degree of correlation perhaps involve distinct time-keeping mechanisms (see Ding et al. 2002). At a more conscious level, shifting patterns of correlation might reflect modified strategy in temporal estimation (see Wagenmakers et al. 2004). And at a systems level, correlation might result when interacting components self-organize at different timescales (see van Orden et al. 2003).

Serial correlations in human performance, such as in threshold discrimination tasks, have been studied for some time (e.g., see Merrill and Bennett 1956; Verplanck et al. 1952; Weiss et al. 1955), and much of the work has led to the conclusion that serial correlations are small and transitory, tending to quickly decay (e.g., Laming 1968, 1979a). However, a certain type of serial dependence (1/f, or 'pink', noise) signals the presence of long-range correlation in a data set, where variability at one time point is correlated with variability at a later point. That is, what a person does on trial 1 may have a direct physical and psychological impact on what that person does on all future trials. Thus, current behavior could be explained by past behavior (Wagenmakers et al. 2004). Other types of long-range correlation, such as 'blue' noise (where variability fluctuates above and below the mean), have been found in addition to 1/f noise in human performance (e.g., in walking stride interval; see Hausdorff et al. 1996). Both types of noise, pink and blue, are distinguished from white noise (i.e., noncorrelated variability).

Recently, Miyazaki et al. (2001) presented evidence that 1/f noise in the initial kinematic markers (i.e., peak acceleration and velocity) of a discrete aiming task was stronger and diminished over the time course of the movement, vanishing when participants reached the target. The authors inferred that, because the function of adjustments for initial kinematic variability seems to be error reduction in final movement amplitude, or increased consistency in total distance traveled (e.g., Gordon and Ghez 1987; Messier and Kalaska 1999), long-range correlation of initial kinematics may reflect the use of adjustment processes early in the movement to increase accuracy later in the movement. In other words, there is assumed to be a positive relationship between early and late characteristics of the movement.¹ The present study will proceed from the notion that such adjustment processes in general serve to reduce variability and, more significantly, will posit that such processes involve coordination between fundamental stages in the movement (i.e., planning and control).

Summation of processes

Thus, to expand on the findings of Miyazaki et al. (2001), we propose that 1/f noise in aiming reflects the operation of both planning and control and that these processes operate at different timescales. As planning tends to be a slower-

¹ Other researchers (e.g., Elliott et al. 1999), using kinematic analysis and sudden perturbations to the movement or the target, have shown that there is sometimes a negative relationship between early and late characteristics of the movement. While these findings help to illuminate the role of effector or target characteristics in the use of adjustment processes, the present study, using fractal time series analysis, will begin from the notion that movement correction (whether early or late) generally serves to reduce variability.

moving process (i.e., movement strategy evolves across trials) and control a faster-moving process (i.e., movement adapts online to local circumstances; see Glover 2004), $1/f$ noise may provide evidence of summation between the two. To illustrate, consider a simple dice-throwing algorithm (Voss as cited in Gardner 1978). Take three dice and throw the first die only rarely, the second die intermittently, and the third die for every observation. Then sum the values for the three dice. This time series will exhibit $1/f$ -like noise. As aiming similarly consists of processes operating at different timescales (i.e., planning vs. control), it is plausible that $1/f$ noise in movement may arise from an analogous superposition of variability.

In the present experiments, the hypothesis was that spatial, physical, and timing constraints would reveal $1/f$ noise beyond the initial stage of movement and that $1/f$ noise would vary throughout movement as a function of time and task. It was predicted that, across experiments, planning and control processes would overlap most during the middle portion of the movement (i.e., at peak velocity), leading to $1/f$ noise.

Experiment 1

This experiment examined aiming movements with varied levels of mass and distance. Kinematic analysis was used to determine how mass and distance affected velocity profiles, while fractal time series analysis was used to examine patterns of variability at certain kinematic markers in the movement trajectory (e.g. time to peak acceleration and velocity) for evidence of time-dependent correlation.

Method

Participants

Twelve undergraduate and three graduate students (10 males and 5 females) at Arizona State University participated in this experiment. Undergraduates participated in exchange for course credit.

Design

Participants performed a discrete aiming task by moving cylindrical objects to targets. There were 16 conditions comprised of four levels of object mass (300, 400, 500, and 600 g) and four target distances (400, 500, 600, and 700 mm).

Apparatus

The apparatus consisted of a 61.0 cm × 122 cm table 76.0 cm in height and four cylindrical objects (7.5 cm in

length, 4.5 cm in diameter), each with a different level of mass. Mass was manipulated with lead shot and foam. There were four red light-emitting diodes, 0.8 cm in height and 0.5 cm in diameter, embedded in the surface of the table. The start point was 12.5 cm from the right edge of the surface. The table was covered with a translucent white cloth to provide a uniform appearance that eliminated any extra visual cues. To record movement, two infrared light-emitting diodes were attached to participants' right index finger and thumb, with an OPTOTRAK 3020 motion-tracking device (Northern Digital, Waterloo, ON, Canada) capturing the signals emitted by these diodes at a sampling rate of 100 Hz.

Procedure

Participants stood approximately 12.0 cm from the right edge of the long side of the table and grasped the object with their right hand. Participants were aware that there would be different target distances and different levels of object mass. Once the experimenter instructed them to do so, participants lifted the object with their right hand, moved the object leftward across the midline of their body, and placed the object on the lit target. The target was lit prior to movement and remained lit until the object reached the target. After participants placed the object on the target, the experimenter removed the object from the table and replaced it with another object at the original start point. There were 80 randomized trials in total. There were no timing constraints on the movement, and no feedback was provided. Participants were allowed to rest if they became fatigued. All procedures were carried out according to the principles of the Helsinki Declaration and were approved by the Institutional Review Board of Arizona State University.

Kinematic analysis

Tangential displacement values for x , y , and z coordinates recorded with the OPTOTRAK were differentiated (i.e., instantaneous rates of change were calculated) to obtain the velocity profile for each movement and differentiated a second time to obtain the acceleration profile. Prior to differentiation, displacement data were filtered with a low-pass Butterworth filter with a cutoff frequency of 12 Hz. Figure 1 illustrates typical profiles for distance, velocity, and acceleration. Time to each kinematic marker (peak acceleration, peak velocity, peak deceleration, and movement end) was measured, as well as temporal variability, or the within-participant standard deviation in time to each kinematic marker (see Khan et al. 2002, who analyzed standard deviation in distance traveled to each kinematic marker).

Time to each kinematic marker was analyzed with a 4 (mass) × 4 (distance) × 4 (kinematic marker) within-participant repeated measures analysis of variance (ANOVA).

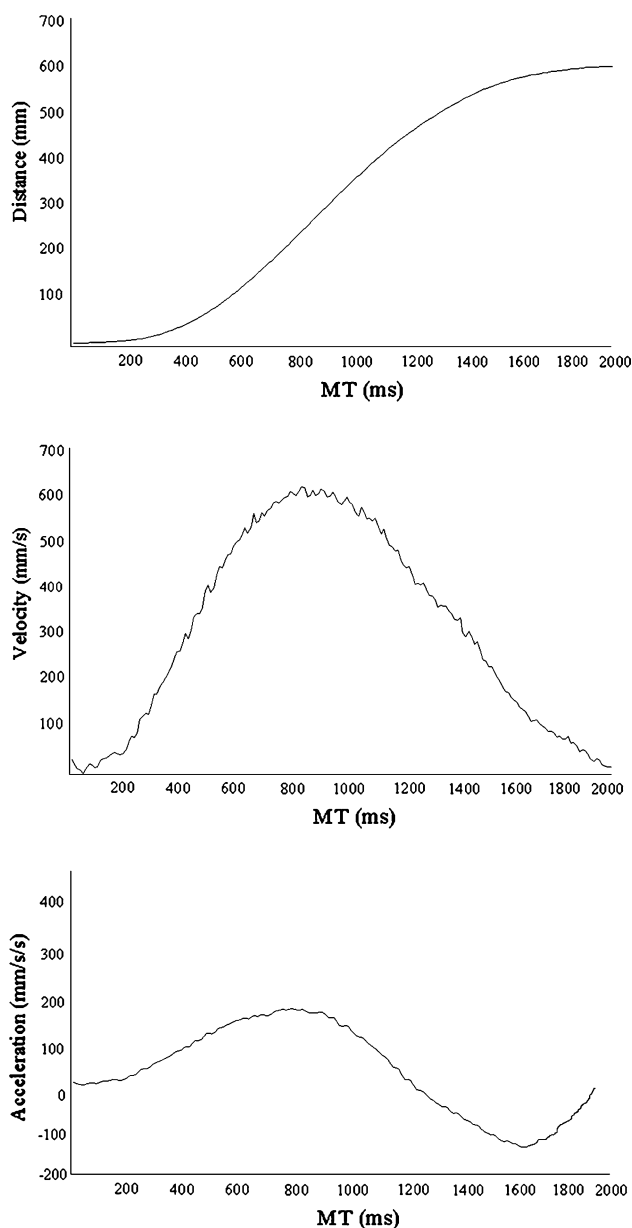


Fig. 1 Typical velocity profiles. From *top to bottom*: distance, velocity, and acceleration as a function of movement time (from Experiment 1)

Temporal variability was analyzed with a 4 (mass) \times 4 (distance) \times 4 (kinematic marker) within-participant repeated measures ANOVA. Interactions were tested via analysis of simple effects. The Greenhouse–Geisser correction was used when the assumption of independence of observations was violated, with corrected degrees of freedom reported where appropriate. A significance criterion of 0.05 was used for all tests.

Fractal time series analysis

Fractal time series analysis was used to determine the degree of long-range correlation in the times to each of the

four kinematic markers across the 80 trials per participant. This was comprised of four analyses: power spectral density (PSD), standardized dispersion, rescaled range (R/S), and autoregressive fractionally integrated moving average (ARFIMA). After subtracting condition means from each time series, these four analyses were used to provide converging evidence of long-range correlation in the data (see Rangarajan and Ding 2000 for discussion of an integrated approach to assessing long-range correlation). The mean autocorrelation function (ACF) at each kinematic marker also was computed to determine the extent to which each signal matched a time-shifted version of itself, based on the amount of the shift [i.e., plotting the value of the autocorrelation $C(k)$ at lag k], providing another measure of the serial structure of each time series.

Power spectral density analysis was used to classify the time series (to determine subsequent analysis) and establish whether it was in the range of $1/f$ noise. From a fast Fourier transform of the data, PSD analysis provided the slope of log power as a function of log frequency, or the spectral index (β), used to determine both signal class and fractal dimension. The fractional Gaussian noise (fGn)/fractional Brownian motion (fBm) dichotomous model was used to define the signal: a fGn signal is stationary, indicating that variance is constant; whereas a fBm signal is nonstationary, indicating that variance increases with time (see Eke et al. 2000, 2002).

After establishing that the data were stationary and in the range of $1/f$ noise, standardized dispersion analysis was used to obtain a converging measure of fractal dimension, D_{Disp} , equivalent to β , where $D_{\text{Disp}} = 1 + (\beta + 1)/2$ (for an overview, see Bassingthwaite 1988; Bassingthwaite and Raymond 1995; Holden 2005). The analysis began by standardizing the raw data (the time to each kinematic marker) using z scores. Then, the standard deviation (SD) of the data was calculated at different levels (or bins) of resolution. The size of the bin (m) refers to the number of adjacent trials over which SD was calculated. So, we began by calculating SD for each non-overlapping adjacent pair ($m = 2$) and then taking the average of those values. This process was repeated for $m = 4, 8, 16$, and 32. The slope of $\log \text{SD}(m)$ as a function of $\log m$ was calculated to determine fractal dimension, D_{Disp} ($D_{\text{Disp}} = 1 - \text{slope}$). As PSD and standardized dispersion analyses yielded similar fractal dimensions, to be consistent, the averaged fractal dimension (the averaged D) across the two analyses was calculated.

After calculating the averaged fractal dimension across PSD and standardized dispersion analyses for each participant at each kinematic marker, a single-sample t test was used to test if mean averaged D was significantly different from 1.50, or white noise. Following Holden (2005), where the averaged D differed from 1.50, 10 surrogate (reshuffled)

data sets were used to confirm that long-range correlation was not random (i.e., the order of the original time series was reshuffled ten times, each time computing the average fractal dimension of each surrogate). To determine the relative degree of correlation at each kinematic marker, where the averaged D differed from 1.50 at more than one kinematic marker, paired t tests were used to test if the averaged D values at these markers were significantly different.

As fractal time series analysis based on only mean values may obscure nonrandom correlation at an individual level (e.g., see Hausdorff et al. 1996), a binomial test also was used to categorize participants by kinematic marker into two groups: those with an averaged D of less than 1.50, signaling $1/f$ noise, and those with an averaged D of 1.50 or greater, signaling either white noise or blue noise (i.e., anti-correlation, or positive values followed by negative values). This test was used to determine whether $1/f$ noise was exhibited by a significant majority at any kinematic marker.

Finally, R/S and ARFIMA were used. R/S is similar to standardized dispersion analysis in that it uses consecutive partitions (bins) on a times series; however, unlike standardized dispersion analysis, R/S compares the range between the largest and smallest values over a partition to the length of that partition (Killeen 2005). This range is then divided by the SD of values in the bin. R/S yielded another converging measure of fractal dimension, the Hurst coefficient (H), estimated using the slope of a linear regression fitted on a $\log(\text{mean } R/S)$ by $\log(\text{length of bin})$ plot equivalent to both β and D_{Disp} , where $D_{\text{Disp}} = 2 - H$. As with the averaged D , a single-sample t test was used to test if mean H was significantly different from 0.50, or white noise; where mean H differed from 0.50, surrogate data sets were used to confirm that long-range correlation was not random; and to determine the relative degree of correlation at each kinematic marker, where mean H differed from 0.50 at more than one kinematic marker, paired t tests were used to test if mean H values at these markers were significantly different.

ARFIMA, on the other hand, estimated long-range correlation by incorporating short-range processes (via the autoregressive parameters p and moving average parameters q) and a long-range process (via the fractional differencing parameter d), where the ARMA (p, q) component described short-range processes; and the d parameter, related to β , D_{Disp} , and H by the equation $\beta = 2d$, quantified the degree of long-range correlation (i.e., when $d = 0$, there was no correlation; when $0 < d < 0.5$, the series was stationary with correlation; when $d \geq 0.5$, the series was non-stationary; see Wagenmakers et al. 2004 for a more comprehensive treatment). An ARFIMA model selection procedure (see Wagenmakers et al. 2005) was used that involved fitting 18 models to each time series at each kinematic marker. Nine of the models were ARMA (p, q) mod-

els, where p and q varied from 0 to 2; the other nine models were the corresponding ARFIMA (p, d, q) models. If long-range correlation was present in the time series, then ARFIMA versus ARMA models would better fit the data, with d significantly different from 0. Basing this test on a wide range of ARFIMA models is important, as correct specification of p and q permits more precise estimation of d (Taqqu and Teverovsky 1998; Wagenmakers et al. 2005).

The Akaike information criterion (AIC: Akaike 1973) and Bayes information criterion (BIC) were used to evaluate the tradeoff between accuracy and parsimony in model selection (i.e., where the best model giving a good account of the data contained a minimum number of free parameters). In the case of AIC, for example, computed according to the equation $\text{AIC} = -2\log L + 2k$, where L is the maximum likelihood of the model and k the number of free parameters plus an additional variance parameter [$k = p + q + 1$ for ARMA (p, q) and $k = p + q + 2$ for ARFIMA (p, d, q)], there is a reward for accuracy in the first term of the AIC and a penalty for lack of parsimony in the second term. Better models are assumed to be characterized by lower AIC values. BIC is similar to AIC, with the exception that BIC, defined as $\text{BIC} = -2\log L + k\log N$, where N is the number of observations in the time series, should more severely penalize complex models (see Torre et al. 2007 for an overview).

After obtaining raw values for both AIC and BIC, these values were transformed into weights (see Wagenmakers and Farrell 2004). To select the best model among m candidates, then, the difference between the criterion for each model and the best model was computed; this difference was converted to an estimate of relative likelihood; and this relative likelihood was normalized into a weight. The resulting weights represented the probability of the i th model being the best model (Wagenmakers and Farrell 2004), where the weights in a given set of models sum to 1. If there was long-range correlation in the data, then the ARFIMA model would have the largest weight, and the sum of the ARFIMA model weights would be greater than the sum of the ARMA model weights. Model fitting was accomplished using the ARFIMA package (Doornik and Ooms 1999; Ooms and Doornik 1998) for the matrix computing language Ox (Doornik 2001).

Results

Kinematic analysis

Mean movement times across kinematic markers are shown in Fig. 2. There were significant effects of distance ($F_{3,42} = 85.66, P < 0.05, \eta^2 = 0.86$) and kinematic marker ($F_{1,21,17,02} = 179.64, P < 0.05, \eta^2 = 0.92$), with a significant distance \times kinematic marker interaction ($F_{1,99,27,95} = 27.32$,

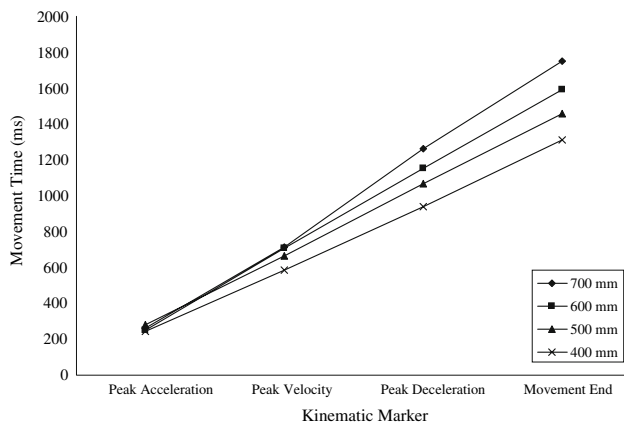


Fig. 2 Experiment 1: Mean movement times (in milliseconds) at each kinematic marker and target distance

$P < 0.05$, $\eta^2 = 0.66$). Simple effects analysis of this interaction showed that there was an increase in time to peak velocity ($F_{3,42} = 23.94$, $P < 0.05$, $\eta^2 = 0.63$), time to peak deceleration ($F_{3,42} = 40.08$, $P < 0.05$, $\eta^2 = 0.74$), and time to movement end ($F_{1,28,17.97} = 73.06$, $P < 0.05$, $\eta^2 = 0.83$) as distance increased from 400 to 700 mm. All other effects were not significant. There were no differences between male and female participants throughout (e.g., see Hansen et al. 2007 for discussion of gender-related differences in the use of planning and control).

Temporal variability across kinematic markers is shown in Fig. 3. There were significant effects of distance ($F_{3,42} = 5.18$, $P < 0.05$, $\eta^2 = 0.27$) and kinematic marker ($F_{3,42} = 9.70$, $P < 0.05$, $\eta^2 = 0.40$), with a significant distance \times kinematic marker interaction ($F_{3,39,47.49} = 3.12$, $P < 0.05$, $\eta^2 = 0.18$). There was a marginally significant linear trend, where variability tended to increase as the movement progressed ($F_{1,14} = 3.51$, $P = 0.08$, $\eta^2 = 0.20$) and a significant quadratic trend ($F_{1,14} = 5.69$, $P < 0.05$, $\eta^2 = 0.28$), where variability decreased after peak deceleration.

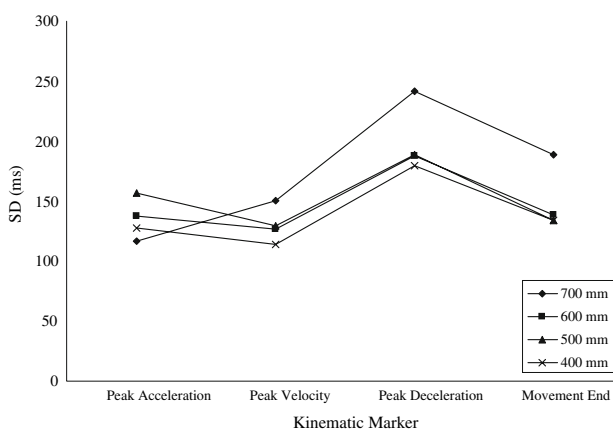


Fig. 3 Experiment 1: Temporal variability (SD in milliseconds) at each kinematic marker and target distance

tion to movement end. This leveling off and collapse in variability toward the end of the movement suggests greater influence of control as the movement unfolded (e.g., see Elliott et al. 2004).

Fractal time series analysis

Figure 4 shows a sample time series. Figures 5 and 6 show the mean ACF and power spectrum, respectively. Table 1 shows mean values for PSD, standardized dispersion, R/S , and ARFIMA. Applying PSD analysis to the data resulted in a mean β of greater than -1 and less than 1 at all four kinematic markers, classifying each signal as fGn, or stationary. As a measure of fractal dimension, the mean β of greater than -1 and less than 0 at all four kinematic markers indicated that the data were in the range of $1/f$ noise (see Eke et al. 2000, 2002).

Standardized dispersion analysis showed that mean D_{Disp} was equal to or greater than 1.20 and less than 1.50 at peak velocity, indicating the presence of $1/f$ noise (see van Orden et al. 2003), but not at the other three kinematic markers. After the averaged fractal dimension across PSD and standardized dispersion analysis was calculated for each participant, a single-sample t test showed that mean averaged D was significantly different from 1.50 at peak velocity [$t(14) = -2.28$, $P < 0.05$] but not at the other three kinematic markers [$t(14) = 0.963$, $P < 0.05$ at peak acceleration; $t(14) = -0.190$, $P < 0.05$, at peak deceleration; $t(14) = 1.82$, $P < 0.05$, at movement end]. Surrogate data sets were significantly different from the original data set at peak velocity, confirming that long-range correlation was not random ($P < 0.05$).

Results of the binomial test were not significant (with a criterion of 12 of the 15 participants needed to define a category), indicating that $1/f$ noise was not exhibited by a significant majority at any kinematic marker. However, a trend began to emerge. Of those participants with an averaged D of less than 1.50 , there were five at peak acceleration, nine at peak velocity, eight at peak deceleration, and four at

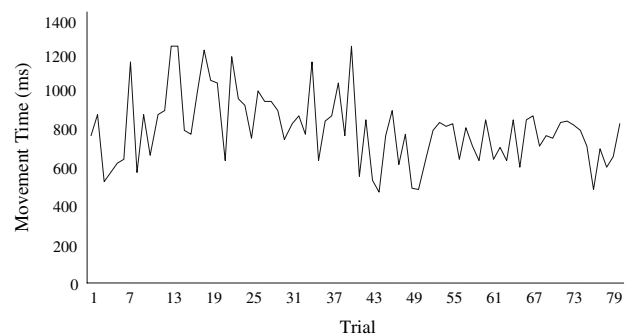


Fig. 4 Experiment 1: Sample time series from one participant (time to peak velocity)

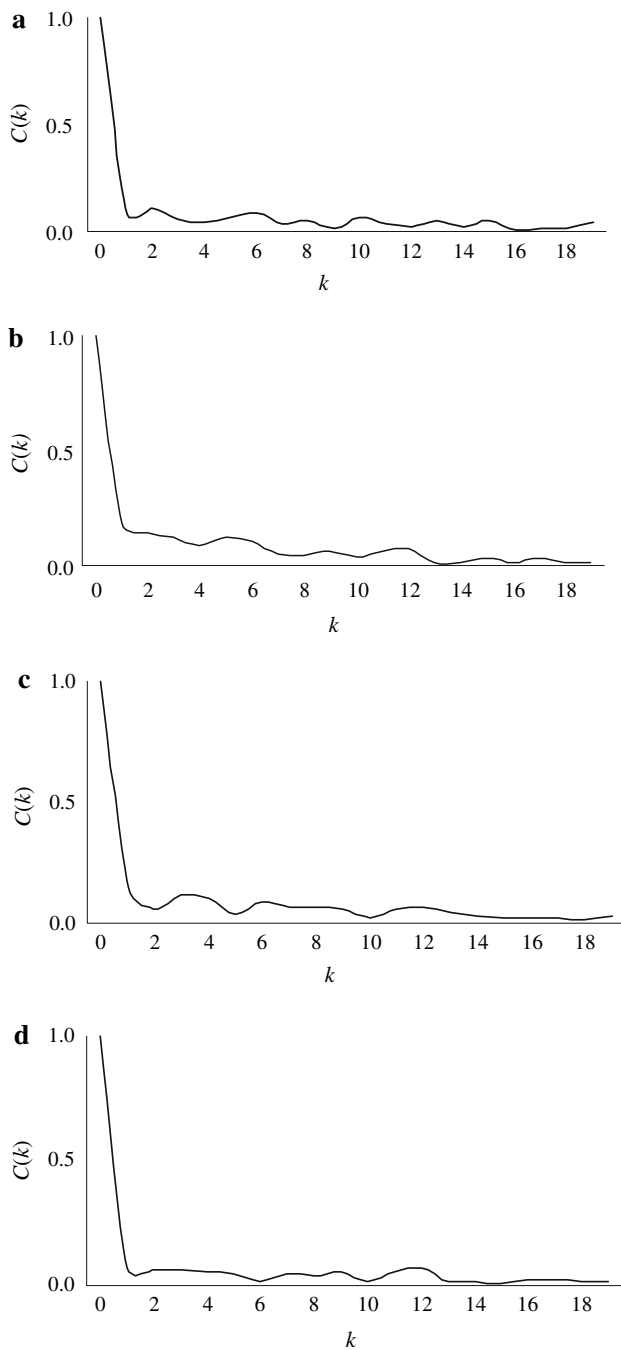


Fig. 5 Experiment 1: Mean autocorrelation function at each kinematic marker. Autocorrelation $C(k)$ as a function of lag k at (a) time to peak acceleration, (b) time to peak velocity, (c) time to peak deceleration, and (d) time to movement end

movement end, suggesting that the occurrence of $1/f$ noise at an individual level was more frequent when planning and control would overlap to the greatest degree (i.e., at peak velocity). As for those participants with an averaged D of 1.50 or greater, ten showed blue noise at peak acceleration, two showed white and four showed blue noise at peak velocity, seven showed blue noise at peak deceleration, and

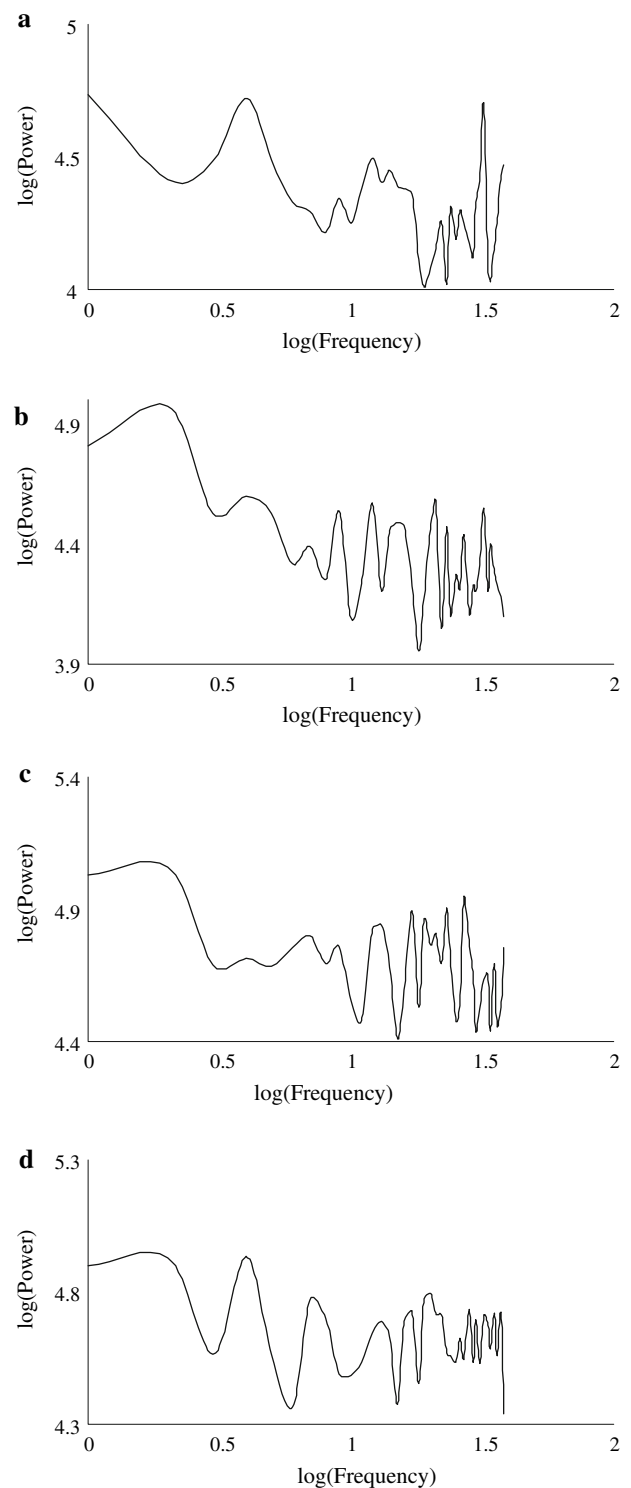


Fig. 6 Experiment 1: Mean power spectrum at each kinematic marker. Log of the power as a function of log of the frequency at (a) time to peak acceleration, (b) time to peak velocity, (c) time to peak deceleration, and (d) time to movement end

one showed white and ten showed blue noise at movement end, suggesting that the occurrence of another type of long-range correlation (i.e., blue noise) at an individual level was

Table 1 Experiment 1: Mean values for PSD, standardized dispersion, *R/S*, and preferred ARFIMA models at each kinematic marker

	Peak acceleration	Peak velocity	Peak deceleration	Movement end
PSD (β)	-0.24 ^a	-0.35 ^a	-0.20 ^a	-0.12 ^a
Standardized Dispersion (D_{Disp})	1.50	1.44 ^a	1.51	1.54
<i>R/S</i> (<i>H</i>)	0.73 ^a	0.80 ^a	0.76 ^a	0.74 ^a
ARFIMA—AIC (<i>d</i>)	0.27 ^b	0.25 ^b	0.29 ^b	0.26 ^b
ARFIMA—BIC (<i>d</i>)	0.24 ^b	0.22 ^b	0.21 ^b	(0.17)

Value within the parentheses indicates a single preferred model

^a Within the range of $1/f$ noise

^b Within the range of $1/f$ noise, where *d* was significantly different from 0

more frequent when a single process would be more prominent (e.g., planning at peak acceleration and control at movement end).

R/S showed that mean *H* was greater than 0.50 and equal to or less than 0.80 at all four kinematic markers, indicating the presence of $1/f$ noise. A single-sample *t* test showed that mean *H* was significantly different from 0.50 at all four kinematic markers [$t(14) = 9.97, P < 0.05$, at peak acceleration; $t(14) = 18.41, P < 0.05$, at peak velocity; $t(14) = 12.98, P < 0.05$, at peak deceleration; $t(14) = 10.50, P < 0.05$, at movement end]. Surrogate data sets were significantly different from the original data set at all four kinematic markers ($P < 0.05$). Furthermore, subsequent paired *t* tests showed that mean *H* at peak velocity was significantly higher than mean *H* at the other three kinematic markers [$t(14) = -3.07, P < 0.05$, vs. peak acceleration; $t(14) = 3.02, P < 0.05$, vs. peak deceleration; $t(14) = 3.55, P < 0.05$, vs. movement end]. These results provided further evidence of long-range correlation in the data and that the degree of correlation was highest at peak velocity. However, results from *R/S* should be interpreted more cautiously than those of PSD and standardized dispersion analyses, as *R/S* tends to yield a biased estimate of fractal dimension (e.g., overestimation of *H* for time series with $H < 0.70$ and underestimation of *H* for $H > 0.70$; see Caccia et al. 1997).

Main results of ARFIMA model selection are shown in Table 2. For peak acceleration, AIC preferred an ARFIMA model for six series (40%), with *d* significantly different from 0; and nine series (60%), with *d* not significantly different from 0. BIC preferred an ARFIMA model for four series (26.7%), with *d* significantly different from 0; and 11 series (73.3%), with *d* not significantly different from 0. The mean weight for the best ARFIMA models (i.e., with a significant *d*) was 0.22 (SD = 0.10) for AIC and 0.55 (SD = 0.13) for BIC, while the mean sum of weights for

Table 2 Experiment 1: ARFIMA models percentage preferred, mean weight of models, and mean sum of weights for AIC and BIC criteria at each kinematic marker

	Peak acceleration	Peak velocity	Peak deceleration	Movement end
Preferred—AIC (%)	40	60	46.7	20
Preferred—BIC (%)	26.7	53.3	33.3	6.6
Mean weight—AIC	0.22	0.22	0.24	0.31
Mean weight—BIC	0.55	0.62	0.64	(0.54)
Mean sum of weights—AIC	0.77	0.73	0.73	0.81
Mean sum of weights—BIC	0.88	0.92	0.86	(0.92)

Where *d* was significantly different from 0

Values within the parentheses indicate a single preferred model

ARFIMA models was 0.77 (SD = 0.10) for AIC and 0.88 (SD = 0.07) for BIC. That the mean sums were reasonably close to 1.00 suggests a greater probability that the ARFIMA model is the best model (see Torre et al. 2007). Estimating *d* from the best model selected among the ARFIMA candidate models resulted in a mean *d* of 0.27 (SD = 0.08) for AIC that corresponds to an *H* value of 0.77 and a mean *d* of 0.24 (SD = 0.13) for BIC that corresponds to an *H* value of 0.74. These mean *H* values were consistent with measures of fractal dimension obtained using the other three time series analyses.

For peak velocity, AIC preferred an ARFIMA model for nine series (60%), with *d* significantly different from 0; and six series (40%), with *d* not significantly different from 0. BIC preferred an ARFIMA model for eight series (53.3%), with *d* significantly different from 0; and seven series (46.7%), with *d* not significantly different from 0. The mean weight for the best ARFIMA models was 0.22 (SD = 0.06) for AIC and 0.62 (SD = 0.13) for BIC, while the mean sum of weights for ARFIMA models was 0.73 (SD = 0.06) for AIC and 0.92 (SD = 0.02) for BIC. Estimating *d* from the best model selected among the ARFIMA candidate models resulted in a mean *d* of 0.25 (SD = 0.08) for AIC that corresponds to an *H* value of 0.75 and a mean *d* of 0.22 (SD = 0.04) for BIC that corresponds to an *H* value of 0.72. These mean *H* values were consistent with measures of fractal dimension obtained using the other three time series analyses.

For peak deceleration, AIC preferred an ARFIMA model for seven series (46.7%), with *d* significantly different from 0; seven series (46.7%), with *d* not significantly different from 0; and an ARMA (2, 0, 1) model for one series (6.60%). BIC preferred an ARFIMA model for five series (33.3%), with *d* significantly different from 0; and ten series (66.7%), with *d* not significantly different from 0. The mean weight for the best ARFIMA models was 0.24

(SD = 0.03) for AIC and 0.64 (SD = 0.02) for BIC, while the mean sum of weights for ARFIMA models was 0.73 (SD = 0.04) for AIC and 0.86 (SD = 0.05) for BIC. Estimating d from the best model selected among the ARFIMA candidate models resulted in a mean d of 0.29 (SD = 0.22) for AIC that corresponds to an H value of 0.79 and a mean d of 0.21 (SD = 0.03) for BIC that corresponds to an H value of 0.71. These mean H values were consistent with measures of fractal dimension obtained using the other three time series analyses.

For movement end, AIC preferred an ARFIMA model for three series (20%), with d significantly different from 0; and 12 series (80%), with d not significantly different from 0. BIC preferred an ARFIMA model for one series (6.60%), with d significantly different from 0; and 14 series (93.4%), with d not significantly different from 0. The mean weight for the best ARFIMA models was 0.31 (SD = 0.24) for AIC, with a weight of 0.54 for BIC, while the mean sum of weights for ARFIMA models was 0.81 (SD = 0.05) for AIC, with a sum of 0.92 for BIC. Estimating d from the best model selected among the ARFIMA candidate models resulted in a mean d of 0.26 (SD = 0.11) for AIC that corresponds to an H value of 0.76 and a d of 0.17 for BIC that corresponds to an H value of 0.67. These mean H values were consistent with measures of fractal dimension obtained using the other three time series analyses.

To summarize, the percentage of preferred ARFIMA models at each kinematic marker was somewhat low, affecting the ability to more strongly conclude that long-range correlation characterizes each time series (see Torre et al. 2007, who suggest rejecting the hypothesis of long-range correlation in the data if the percentage of preferred ARFIMA models is less than 70% using AIC and less than 90% using BIC). Nevertheless, the higher percentage (60% for AIC and 53.3% for BIC) of preferred ARFIMA models at peak velocity suggested greater frequency of long-range correlation at this kinematic marker. Also, given the mean sums of the ARFIMA weights (Torre et al. 2007 again suggested threshold values for long-range correlation of approximately 0.70 for AIC and 0.90 for BIC), the reasonable correspondence between d and other obtained measures of fractal dimension, and the observation that only 1 of the 60 total time series was classified as an ARMA process by either AIC or BIC criteria, these results further suggested the likelihood of long-range correlation in the data.

Discussion

Historically, kinematic analysis has been used to make general inferences about planning and control. For example, the initial selection of a movement parameter, such as velocity (reflected in a particular velocity profile), would be viewed as evidence of a plan, while the in-flight adjustment

of this parameter (reflected in changes to the shape of that profile) would be viewed as evidence of control (see Glover 2004 for an overview). Kinematic analysis in the present experiment showed that, with no time constraint, there was no effect of mass and that temporal variability continued to increase from peak acceleration to peak deceleration, after which it decreased, suggesting greater influence of control (e.g., see Elliott et al. 2004).

Like kinematic analysis, fractal time series analysis focuses on the temporal aspects of movement. However, fractal time series analysis provides a method of examining how a movement parameter, such as time to peak velocity, might be autocorrelated as the movement progresses (reflected in a particular pattern of correlation across trials, e.g., $1/f$ noise) and permits further inferences about the time course of parameter selection (i.e., planning) and parameter adjustment (i.e., control). Fractal time series analysis in the present experiment, based first on mean averaged fractal dimension, showed that $1/f$ noise was exhibited only at peak velocity. R/S , based on mean H , further showed that the intensity of $1/f$ noise was greatest at peak velocity. And ARFIMA, based on the long-range parameter d , showed that ARFIMA models were preferred more frequently at peak velocity versus the other kinematic markers. Results from these separate analyses suggest that long-range correlation occurred—and was most prominent—at a time in the movement when adjustments for early variability were not separate from but coordinated with adjustments for later variability. As $1/f$ -like noise has been produced by summing short-range processes at different timescales (Gardner 1978), and planning tends to be slower and control faster, the prominence of $1/f$ noise at peak velocity may provide evidence of an analogous summation of processes.

To further highlight peak velocity, a binomial test, although not significant, also revealed an emerging trend: of those participants with an averaged fractal dimension of less than 1.50, there were more at peak velocity than at the other three kinematic markers. This suggests that the occurrence of $1/f$ noise at an individual level was more frequent when planning and control would perhaps coordinate to the greatest degree. The binomial test revealed another emerging trend, however: of those participants with an averaged fractal dimension of greater than 1.50, there were more showing blue noise at peak acceleration and movement end. This suggests that the occurrence of this other type of long-range correlation at an individual level was more frequent when a single process would be more prominent. Blue noise bears further mention, as it has been found in addition to $1/f$ noise in other types of human performance (e.g., stride-to-stride fluctuations in human locomotion at preferred speed; see Hausdorff et al. 1996, re-analyzed at an individual level by Scafetta et al. 2003).

In the Hausdorff et al. (1996) study, four of the ten participants continually shifted their stride interval, longer and shorter around an average. In the present study, a similar pattern of blue noise was observed systematically (10 of 15 participants at peak acceleration and 10 of 15 at movement end), perhaps reflecting a feature of variability in repeated arm movements that involves an analogous shifting—that of force and timing. To illustrate, the impulse-timing hypothesis posits that a generalized motor program (i.e., an abstract representation that initiates and adjusts a coordinated movement sequence; see Schmidt and Lee 2005) specifies when the muscles become active/inactive and the degree of force to use, thereby controlling impulses, or bursts of force, over time.

Thus, it may be that blue noise occurred as participants continued to calibrate their movement at peak acceleration and movement end on a trial-by-trial basis across all trials; that is, movement that was ‘too fast’ with ‘too much force’ on one trial was followed by movement that was ‘too slow’ with ‘not enough force’ on the next trial. This shifting between faster and slower movements would then fluctuate around an average level of force and timing.

Experiment 2

This experiment examined how a time-minimization constraint interacted with mass and distance to influence movement. When feedback loops (i.e., visual and proprioceptive) have less time to operate, control will have less influence, and there will be greater reliance on planning as the movement unfolds. Thus, it was predicted that there would be less evidence of superposed processes, or less prominent occurrence of $1/f$ noise. As in Experiment 1, kinematic analysis was used to determine how mass and distance affected velocity profiles, while fractal time series analysis was used to examine patterns of variability at certain kinematic markers in the movement trajectory.

Method

Participants

Twelve undergraduate and two graduate students (8 males and 7 females) at Arizona State University participated in this experiment. Undergraduates participated in exchange for course credit.

Design and procedure

The design used in Experiment 1 was the same as that of Experiment 2, and the procedure was the same, with the exception that participants moved as quickly as possible.

Analysis

The analyses used in Experiment 2 were the same as those of Experiment 1.

Results

Kinematic analysis

Mean movement times across kinematic markers are shown in Fig. 7. There were significant effects of mass ($F_{3,39} = 13.84$, $P < 0.05$, $\eta^2 = 0.53$), distance ($F_{3,39} = 71.13$, $P < 0.05$, $\eta^2 = 0.85$), and kinematic marker ($F_{1,25,15.01} = 449.09$, $P < 0.05$, $\eta^2 = 0.97$), with a significant mass \times kinematic marker ($F_{3,99,47.99} = 7.04$, $P < 0.05$, $\eta^2 = 0.32$) interaction. Simple effects analysis of this interaction showed that, as mass increased from 300 to 600 g, mean movement time increased from 133.45 to 156.10 ms at peak acceleration ($F_{2,12,27.60} = 8.32$, $P < 0.05$, $\eta^2 = 0.39$); 313.23 to 348.32 ms at peak velocity ($F_{3,39} = 15.06$, $P < 0.05$, $\eta^2 = 0.53$); 525.55 to 568.90 ms at peak deceleration ($F_{3,39} = 8.85$, $P < 0.05$, $\eta^2 = 0.40$); and 750.86 to 759.86 ms at movement end ($F_{3,39} = 7.90$, $P < 0.05$, $\eta^2 = 0.37$). All other effects were not significant. There were no differences between male and female participants throughout.

Temporal variability across kinematic markers is shown in Fig. 8. There was a significant effect of kinematic marker ($F_{1,66,21.69} = 36.81$, $P < 0.05$, $\eta^2 = 0.73$). In contrast to Experiment 1, there was a significant linear trend, where variability increased as the movement progressed ($F_{1,14} = 66.35$, $P < 0.05$, $\eta^2 = 0.83$), but there was no significant quadratic trend ($F_{1,14} = 1.34$, $P < 0.05$, $\eta^2 = 0.09$). This lack of a collapse in variability after peak deceleration suggests less influence of control as the movement unfolded (e.g., see Elliott et al. 2004), and smaller variability at each kinematic marker compared to Experiment 1 further suggests less overall reliance on control.

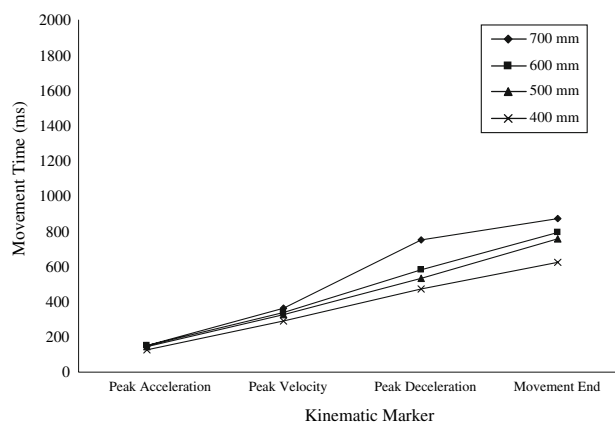


Fig. 7 Experiment 2: Mean movement times (in milliseconds) at each kinematic marker and target distance

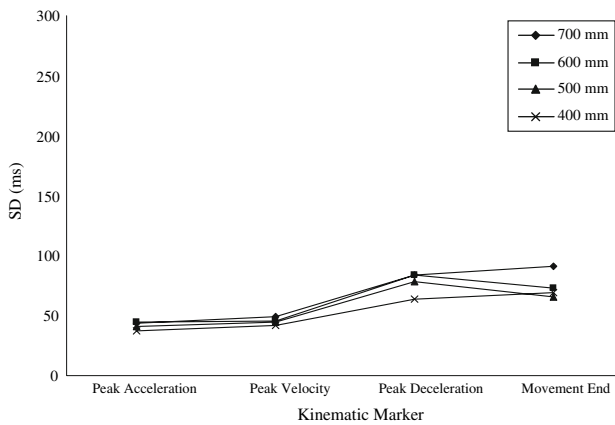


Fig. 8 Experiment 2: Temporal variability (SD in milliseconds) at each kinematic marker and target distance

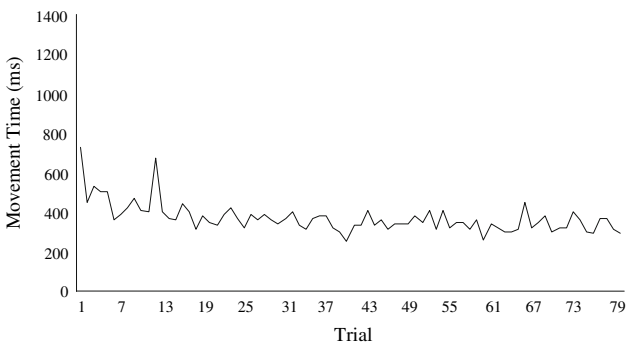


Fig. 9 Experiment 2: Sample time series from one participant (time to peak velocity)

Fractal time series analysis

Figure 9 shows a sample time series. Figures 10 and 11 show the mean ACF and power spectrum, respectively. Table 3 shows mean values for PSD, standardized dispersion, R/S , and ARFIMA. Similar to Experiment 1, applying PSD analysis to the data resulted in a mean β of greater than -1 and less than 1 at all four kinematic markers, classifying each signal as fGn, or stationary. As a measure of fractal dimension, the mean β of greater than -1 and less than 0 at all four kinematic markers indicated that the data were in the range of $1/f$ noise.

Standardized dispersion analysis showed that mean D_{Disp} was not equal to or greater than 1.20 and less than 1.50 at any of the four kinematic markers, indicating an absence of $1/f$ noise. After the averaged fractal dimension across PSD and standardized dispersion analysis was calculated for each participant, a single-sample t test also showed that mean averaged D was not significantly different from 1.50 at any of the four kinematic markers [$t(14) = 0.946$, $P < 0.05$, at peak acceleration; $t(14) = 0.224$, $P < 0.05$, at peak velocity; $t(14) = 0.931$, $P < 0.05$, at peak deceleration; $t(14) = 0.685$, $P < 0.05$, at movement end].

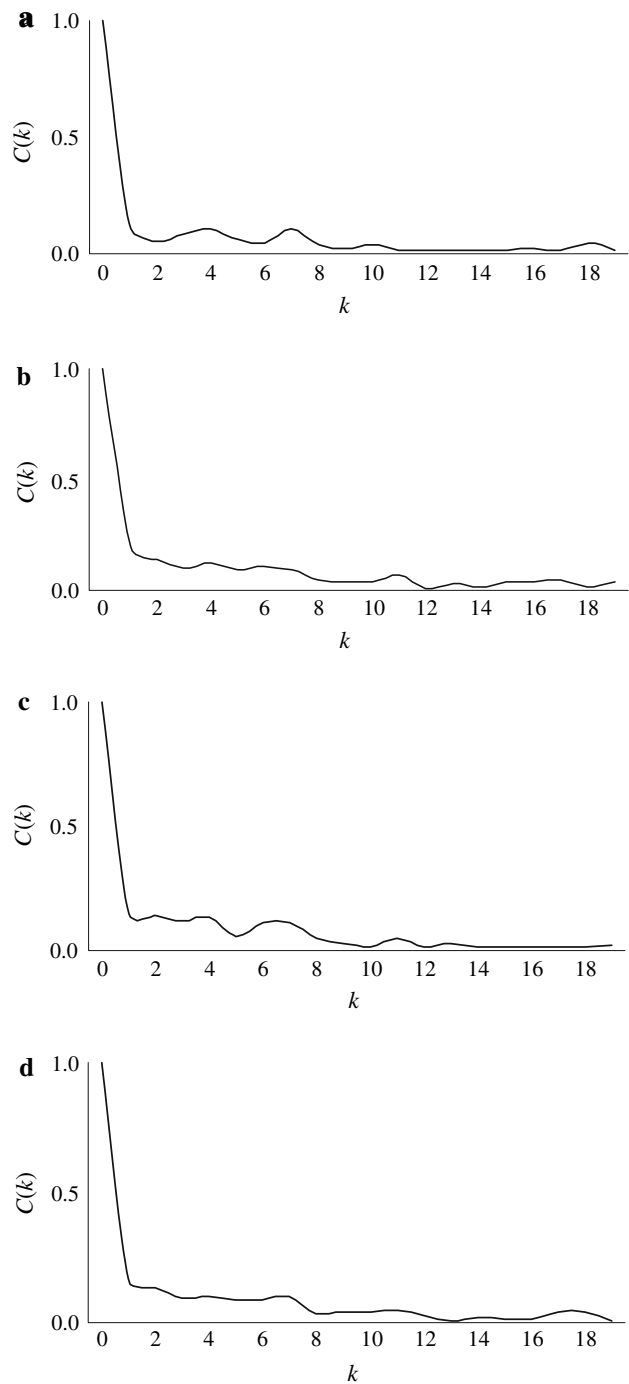


Fig. 10 Experiment 2: Mean autocorrelation function at each kinematic marker. Autocorrelation $C(k)$ as a function of lag k at (a) time to peak acceleration, (b) time to peak velocity, (c) time to peak deceleration, and (d) time to movement end

Results of the binomial test were not significant (with a criterion of 11 of the 14 participants needed to define a category), indicating that $1/f$ noise was not exhibited by a significant majority at any kinematic marker. However, in contrast to Experiment 1, of those participants with an averaged D of less than 1.50 , there were seven at peak accelera-

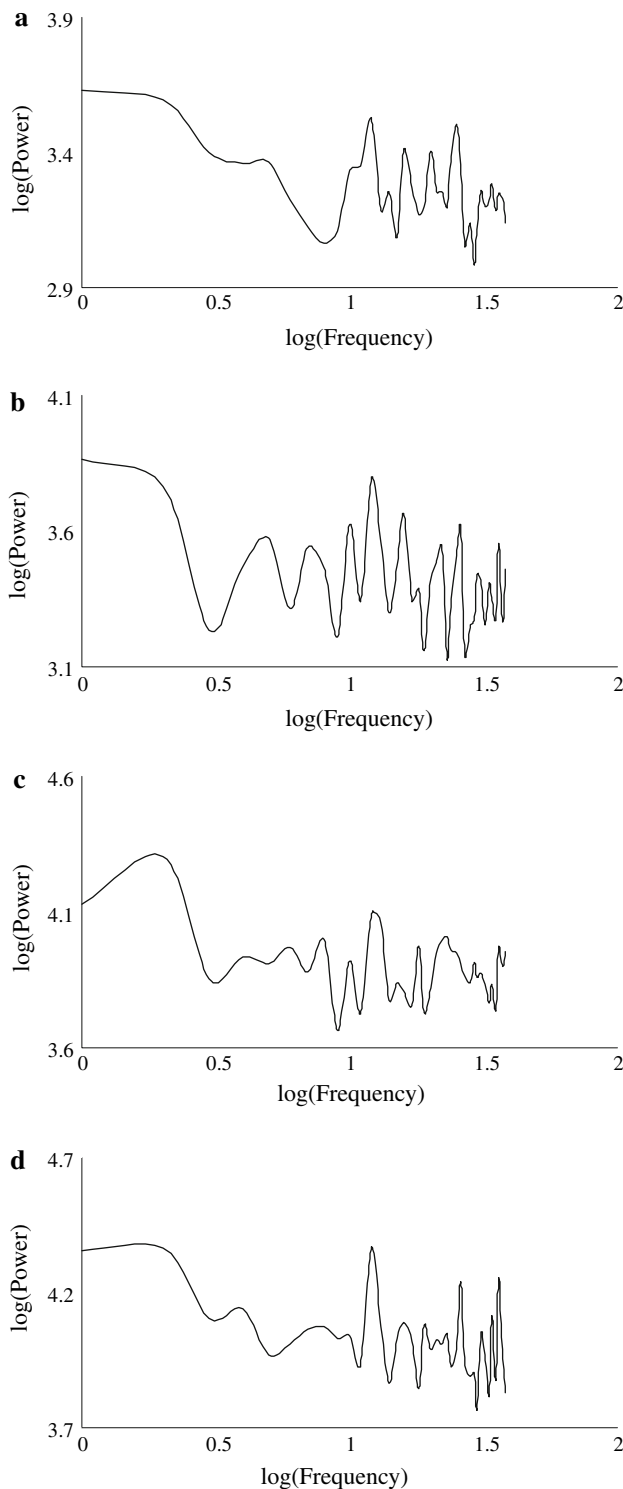


Fig. 11 Experiment 2: Mean power spectrum at each kinematic marker. Log of the power as a function of log of the frequency at (a) time to peak acceleration, (b) time to peak velocity, (c) time to peak deceleration, and (d) time to movement end

tion, eight at peak velocity, seven at peak deceleration, and seven at movement end. This suggests that $1/f$ noise may not have become prominent at peak velocity because there

Table 3 Experiment 2: Mean values for PSD, standardized dispersion, R/S , and preferred ARFIMA models at each kinematic marker

	Peak acceleration	Peak velocity	Peak deceleration	Movement end
PSD (β)	-0.20 ^a	-0.20 ^a	-0.13 ^a	-0.21 ^a
Standardized				
Dispersion (D_{Disp})	1.60	1.51	1.53	1.53
R/S (H)	0.73 ^a	0.78 ^a	0.77 ^a	0.76 ^a
ARFIMA—AIC (d)	0.25 ^b	0.26 ^b	0.32 ^b	0.25 ^b
ARFIMA—BIC (d)	0.23 ^b	0.30 ^b	0.20 ^b	0.25 ^b

^a Within the range of $1/f$ noise

^b Within the range of $1/f$ noise, where d was significantly different from 0;

was not enough time for planning and control to significantly overlap. As for those participants with an averaged D of 1.50 or greater, two showed white and five showed blue noise at peak acceleration, six showed blue noise at peak velocity, seven showed blue noise at peak deceleration, and seven showed blue noise at movement end.

R/S showed that mean H was greater than 0.50 and equal to or less than 0.80 at all four kinematic markers, indicating the presence of $1/f$ noise. A single-sample t test showed that mean H was significantly different from 0.50 at all four kinematic markers [$t(14) = 8.31$, $P < 0.05$, at peak acceleration; $t(14) = 11.12$, $P < 0.05$, at peak velocity; $t(14) = 10.42$, $P < 0.05$, at peak deceleration; $t(14) = 9.14$, $P < 0.05$, at movement end]. Surrogate data sets were significantly different from the original data set at all four kinematic markers ($P < 0.05$). These results provided further evidence of long-range correlation in the data. As in Experiment 1, however, results from R/S should be interpreted more cautiously than those of PSD and standardized dispersion analyses, as R/S tends to yield a biased estimate of fractal dimension.

Main results of ARFIMA model selection are shown in Table 4. For peak acceleration, AIC preferred an ARFIMA model for eight series (57.1%), with d significantly different from 0; and six series (42.9%), with d not significantly different from 0. BIC preferred an ARFIMA model for five series (35.7%), with d significantly different from 0; and nine series (64.3%), with d not significantly different from 0. The mean weight for the best ARFIMA models was 0.27 (SD = 0.13) for AIC and 0.56 (SD = 0.17) for BIC, while the mean sum of weights for ARFIMA models was 0.75 (SD = 0.06) for AIC and 0.84 (SD = 0.10) for BIC. That the mean sums were reasonably close to 1.00 suggests a greater probability that the ARFIMA model is the best model. Estimating d from the best model selected among the ARFIMA candidate models resulted in a mean d of 0.25 (SD = 0.04) for AIC that corresponds to an H value of 0.75 and a mean d of 0.23 (SD = 0.04) for BIC that corresponds to an H value

Table 4 Experiment 2: ARFIMA models percentage preferred, mean weight of models, and mean sum of weights for AIC and BIC criteria at each kinematic marker

	Peak acceleration	Peak velocity	Peak deceleration	Movement end
Preferred—AIC (%)	57.1	14.3	28.6	21.4
Preferred—BIC (%)	35.7	14.3	21.4	35.7
Mean weight—AIC	0.27	0.26	0.22	0.16
Mean weight—BIC	0.56	0.55	0.65	0.46
Mean sum of weights—AIC	0.75	0.75	0.69	0.66
Mean sum of weights—BIC	0.84	0.88	0.87	0.83

Where d was significantly different from 0

of 0.73. These mean H values were consistent with measures of fractal dimension obtained using PSD and R/S analyses.

For peak velocity, AIC preferred an ARFIMA model for two series (14.3%), with d significantly different from 0; and 12 series (85.7%), with d not significantly different from 0. BIC preferred an ARFIMA model for two series (14.3%), with d significantly different from 0; and 12 series (85.7%), with d not significantly different from 0. The mean weight for the best ARFIMA models was 0.26 (SD = 0.02) for AIC and 0.55 (SD = 0.24) for BIC, while the mean sum of weights for ARFIMA models was 0.75 (SD = 0.04) for AIC and 0.88 (SD = 0.08) for BIC. Estimating d from the best model selected among the ARFIMA candidate models resulted in a mean d of 0.26 (SD = 0.02) for AIC that corresponds to an H value of 0.76 and a mean d of 0.30 (SD = 0.03) for BIC that corresponds to an H value of 0.80. These mean H values were consistent with measures of fractal dimension obtained using PSD and R/S analyses.

For peak deceleration, AIC preferred an ARFIMA model for four series (28.6%), with d significantly different from 0; nine series (64.3%), with d not significantly different from 0; and an ARMA (2, 0, 2) model for one series (7.10%). BIC preferred an ARFIMA model for three series (21.4%), with d significantly different from 0; and 11 series (78.6%), with d not significantly different from 0. The mean weight for the best ARFIMA models was 0.22 (SD = 0.02) for AIC and 0.65 (SD = 0.03) for BIC, while the mean sum of weights for ARFIMA models was 0.69 (SD = 0.02) for AIC and 0.87 (SD = 0.04) for BIC. Estimating d from the best model selected among the ARFIMA candidate models resulted in a mean d of 0.32 (SD = 0.24) for AIC that corresponds to an H value of 0.82 and a mean d of 0.20 (SD = 0.05) for BIC that corresponds to an H value of 0.70. These mean H values were consistent with measures of fractal dimension obtained using PSD and R/S analyses.

For movement end, AIC preferred an ARFIMA model for three series (21.4%), with d significantly different from

0; eight series (57.2%), with d not significantly different from 0; and an ARMA (1, 0, 1 and 2, 0, 2) model for three series (21.4%). BIC preferred an ARFIMA model for five series (35.7%), with d significantly different from 0; and nine series (64.3%), with d not significantly different from 0. The mean weight for the best ARFIMA models was 0.16 (SD = 0.02) for AIC and 0.46 (SD = 0.08) for BIC, while the mean sum of weights for ARFIMA models was 0.66 (SD = 0.09) for AIC and 0.83 (SD = 0.08) for BIC. Estimating d from the best model selected among the ARFIMA candidate models resulted in a mean d of 0.25 (SD = 0.03) for AIC that corresponds to an H value of 0.75 and a mean d of 0.25 (SD = 0.02) for BIC that corresponds to an H value of 0.75. These mean H values were consistent with measures of fractal dimension obtained using PSD and R/S analyses.

To summarize, as in Experiment 1, the percentage of preferred ARFIMA models at each kinematic marker was somewhat low, affecting the ability to more strongly conclude that long-range correlation characterizes each time series. Nevertheless, the lower percentage (14.3% for both AIC and BIC) of preferred ARFIMA models at peak velocity compared to Experiment 1 suggested lesser frequency of long-range correlation at this kinematic marker. Also, given the mean sums of the ARFIMA weights, the reasonable correspondence between d and two of the other three obtained measures of fractal dimension, and the observation that only 4 of the 56 total time series were classified as an ARMA process by either AIC or BIC criteria, these results further suggested the likelihood of long-range correlation in the data.

Discussion

Kinematic analysis showed that, with a time-minimization constraint, there were effects of mass and kinematic marker. That is, participants took more time to reach each kinematic marker as the mass of the object increased. Compared to Experiment 1, perhaps these increased movement times reflected incomplete load compensation and, on a biomechanical level, the prolonged activation of agonist muscle groups and delayed response of antagonist muscle groups in response to the added mass (see Smeets et al. 1990). Also, in contrast to Experiment 1, temporal variability continued to increase from peak acceleration to peak deceleration but did not significantly decrease to movement end, suggesting less influence of control (e.g., see Elliott et al. 2004).

As movement times in Experiment 2 did not preclude the use of control processes, it bears mentioning that previous research suggests two types of online control: early in the movement, involving comparison between dynamic properties of the limb (e.g., velocity) and some internal representation of anticipated physical consequences (e.g.,

expected velocity; see Wolpert and Ghahramani 2000; Wolpert et al. 1995); and later in the movement, involving comparison between limb and target position (see Woodworth 1899). Perhaps in Experiment 2, fewer participants were able to smoothly integrate early control processes and generate a reliable representation of the movement—evidenced by less frequent occurrence of $1/f$ noise at peak velocity—while more participants attempted to integrate control at the end of the movement, where the continuously lit target would allow for more sustained comparison between the limb and endpoint.

There also was smaller variability at each kinematic marker. This latter result is perhaps related to the observation that, with faster movement, timing is more accurate, while conversely, timing is less accurate with slower movement (Newell et al. 1979). Such a controversial finding (see Plamondon and Alimi 1997), where temporal variability decreases with decreased MT, appears less controversial when viewed in terms of cooperation between planning and control: less temporal variability as the movement unfolds means less reliance on control and hence more exclusive planning.

Fractal time series analysis, based first on mean averaged fractal dimension, showed that $1/f$ noise was not exhibited at any of the four kinematic markers. However, R/S , based on mean H , showed $1/f$ noise at all four kinematic markers and that the intensity of $1/f$ noise was greater at peak velocity than at peak acceleration and peak deceleration. And importantly, ARFIMA, based on the long-range parameter d , further showed that ARFIMA models were preferred less frequently at peak velocity compared to Experiment 1. Thus, although results based on mean averaged fractal dimension are incongruent with subsequent analyses, overall results still suggest that long-range correlation occurred throughout the movement, with less $1/f$ noise at peak velocity offering less evidence of summation of processes, as the time-minimization constraint may have left insufficient time for planning and control to coordinate significantly at this kinematic marker.

To underscore the effects of the time-minimization constraint (and the decreased influence of control), the binomial test, although not significant, revealed that of those participants with an averaged fractal dimension of less than 1.50, there was only one more at peak velocity than at the other three kinematic markers. This suggests that participants did not have sufficient time to smoothly integrate planning and control processes, as in Experiment 1. It may be that the relatively equal occurrence of $1/f$ noise at peak deceleration and movement end reflects some participants' attempt to engage more control in spite of having less time to do so, whereas the equally frequent occurrence of blue noise at these same kinematic markers reflects other participants' greater reliance on a single process (i.e., planning).

General discussion

$1/f$ noise previously had been shown to occur during the initial stage of a discrete aiming task (Miyazaki et al. 2001). However, this correlation was observed using only one target distance, constant mass, and with participants moving as quickly as possible. The present experiments took into account the spatial, physical, and timing constraints in most common situations and showed that target distance, mass, and timing affect movement trajectory and that long-range correlation occurs throughout the movement, changing by time and task.

$1/f$ Noise: coordination leads to correlation

Planning and control are two fundamental stages of movement that overlap through time (see Desmurget and Grafton 2000; Wolpert and Ghahramani 2000; Wolpert et al. 1995), and it is assumed that planning is totally responsible for determining initial movement parameters while control exerts greater influence as the movement unfolds. Thus, each stage will influence the movement as a function of time (see Glover 2004), and the present study took the perspective that the crossover between planning and control signals coordination between the two stages.

The study of $1/f$ noise in movement variability offers a new perspective on this likely coordination between planning and control. Miyazaki et al. (2001) discovered long-range correlation in an aiming task and inferred that its attenuation through time reflected adjustment processes mainly in the initial kinematics of the movement. The present experiments expanded on the Miyazaki et al. (2001) study to show that patterns of correlation reflect adjustment processes not just in initial kinematics, but throughout the trajectory, as a function of both time and task; and that there may indeed be a time- and context-dependent cooperation between planning and control processes.

Slower- and faster-moving processes in movement

Planning typically evolves across trials, and control typically responds to immediate uncertainty within trials. In the present experiments, when planning and control processes would have overlapped most (at peak velocity), variability in planning might have been superposed with variability in control to produce the observed $1/f$ noise. Conversely, when there was less frequent occurrence of $1/f$ noise, as a result of there being less time for both planning and control, this would suggest less coordination between the two processes.

The present study referenced Voss's dice algorithm (cited in Gardner 1978), where variability in short-range processes was superposed to produce $1/f$ -like noise, to illustrate the

plausibility of $1/f$ noise in movement arising from an analogous superposition of variability. And given the emerging trend of correlation in Experiment 1—a tendency toward more frequent occurrence of $1/f$ noise at peak velocity—the dice analogy is taken further: perhaps $1/f$ noise in movement is the synthesis of the less ordered information of local circumstances processed by control [the white noise at the peripheries of our nervous system (Mandelbrot cited in Gardner 1978)] and the more ordered information of a movement strategy processed by planning that takes place when the two processes coordinate. This would represent a special case of a broader perceptual phenomenon (e.g., perception of music) through which the ‘changing content of our total experience’ (Gardner 1978) clusters around $1/f$ noise. Present results, however, do not provide conclusive evidence for such a definitive interpretation, as the absence of clear statistical significance in the binomial test for each experiment calls for caution in drawing stronger inferences about the distribution of $1/f$ noise; and just as important to recognize, the length of each time series could have affected estimates of $1/f$ noise. This latter point in particular bears further discussion.

Time series length

Physiological research has led to the conclusion that fractal time series methods fail to yield reliable results based on series shorter than 2^{12} data points (e.g., see Caccia et al. 1997; Eke et al. 2000, 2002); series shorter than this may result in unacceptably high levels of bias and variability in estimating long-range correlation. In psychological research, however, this length of time series typically cannot be collected (see Delignieres et al. 2006 for an overview). That is, the lengthening of a typical psychological task (such as the one used in the present experiments) may produce significant problems regarding fatigue or loss of concentration (Madison 2001), undermining the assumption in time series analyses that the system examined does not change throughout the course of observation. So while it is crucial, from an analytical perspective, to strive for acceptable levels of bias and variability in estimating long-range correlation (e.g., see Delignieres et al. 2006) and to reliably distinguish short- from long-range processes (e.g., avoiding spurious measures of long-range correlation by correctly identifying short-range processes; see Wagenmakers et al. 2004), both facilitated by the use of longer time series; from a psychological perspective, it is important to recognize that certain processes (e.g., planning and control of movement) and the coordination between those processes are perhaps maximized on the order of minutes and even milliseconds, possibilities that may warrant consideration of more moderate-length time series.

Accordingly, some researchers have suggested that an acceptable compromise in time series length involves the

use of 2^9 or 2^{10} data points. This suggestion stems largely from experiments using tasks such as finger tapping or synchronization (e.g., see Chen et al. 1997; Musha et al. 1985; Yamada 1996; Yamada and Yonera 2001), tasks that fall under a continuous movement paradigm. A discrete movement paradigm, by contrast, has involved the use of even shorter time series (of approximately 2^8 data points) to obtain measures of long-range correlation (e.g., Miyazaki et al. 2001, who had participants point to a single target using one level of mass and distance), where parsing of consistent ballistic trajectories to examine planning and control processes is critical. Such a paradigm is perhaps particularly sensitive to additional parameters (e.g., increases in mass and distance) that may further contribute to fatigue or diminished concentration. As we included these additional parameters in the present study, and weighed their possible effect on the viability of the data, this certainly factored into the use of the present number of data points.

We must be clear in pointing out that longer time series are generally advisable and that present results should be interpreted in light of any potential limitations posed by such shorter series (e.g., a possible increase in variability in estimates of long-range correlation or less reliable distinction between short- and long-range processes). In being cautious, however, we must also note that simulation studies using classical fractal analysis methods (e.g., Delignieres et al. 2006, who simulated series ranging from 2^6 to 2^{11} data points) have shown that although variability of fractal estimates generally increases with decreased series length, mean fractal estimates tend to remain relatively stable. Simulation studies using ARFIMA modeling (e.g., Torre et al. 2007, who simulated series ranging from 2^7 to 2^{11} data points) have produced somewhat similar (if more complex) results: variability of fractal estimates likewise tends to increase with shorter series, using both AIC and BIC criteria, with mean fractal estimates based on BIC remaining more stable for short series (e.g., down to 2^8 data points) compared to those estimates based on AIC. Thus, whether from empirical or simulated studies, the aforementioned findings highlight the notion that a significant future aim in this paradigm will be the development of methods for obtaining longer, viable time series (that yield stable levels of both bias and variability in fractal estimates) for a broader spectrum of psychological tasks.

Summary

In Experiment 1 (moving at preferred speed) of the present study, of those participants who showed $1/f$ noise, more tended to show $1/f$ noise at peak velocity. $1/f$ -like noise has been produced by summing short-range processes at different timescales (Gardner 1978), and as planning tends to be

a slower-moving process and control faster, present results offer initial evidence that $1/f$ noise in aiming with multiple constraints may arise from a similar summation of short-range processes. In Experiment 2 (moving as quickly as possible), however, of those participants who showed $1/f$ noise, there was less frequent occurrence of $1/f$ noise at peak velocity, perhaps because planning and control did not have sufficient time to overlap. Although results from both experiments offer evidence that $1/f$ noise in aiming may be time and task dependent, these results must be interpreted with some caution, as the length of each time series may have posed certain limitations on estimates of $1/f$ noise, and the degree of long-range correlation in participants' movement may have depended on a range of parameters in addition to those examined.

Acknowledgments The authors gratefully acknowledge the contributions of Peter Killeen, Stephen Goldinger, and Didier Delignieres. This research was supported by National Science Foundation grant BCS-0518013.

References

- Akaike H (1973) Information theory and an extension of maximum likelihood principle. In: Petrov BN, Csaki F (eds) Proceedings of the 2nd international symposium on information theory. Akademiai Kiado, Budapest
- Bassingthwaight J (1988) Physiological heterogeneity: fractals link determinism and randomness in structures and functions. *News Physiol Sci* 3:5–10
- Bassingthwaight J, Raymond G (1995) Evaluation of the dispersional analysis method for fractal time series. *Ann Biomed Eng* 23:491–505
- Caccia DC, Percival DB, Cannon MJ, Raymond GM, Bassingthwaight JB (1997) Analyzing exact fractal time series: evaluating dispersional analysis and rescaled range methods. *Physica A* 246:609–632
- Chen Y, Ding M, Kelso JAS (1997) Long memory processes ($1/f$ type) in human coordination. *Phys Rev Lett* 79:4501–4504
- Delignieres D, Ramdani S, Lemoine L, Torre K, Fortes M, Ninot G (2006) Fractal analyses for 'short' time series: a re-assessment of classical methods. *J Math Psychol* 50:525–544
- Desmurget M, Grafton S (2000) Forward modeling allows feedback control for fast reaching movements. *Trends Cogn Sci* 11:423–431
- Ding M, Chen Y, Kelso JA (2002) Statistical analysis of timing errors. *Brain Cogn* 48:98–106
- Doornik JA (2001) Ox: an object-oriented matrix language. Timberlake Consultants Press, London
- Doornik JA, Ooms M (1999) A package for estimating, forecasting, and simulating Arfima models: Arfima package 1.0 for Ox. <http://www.doornik.com/download/arfima.pdf>
- Eke H, Bassingthwaight J, Raymond G, Percival D, Cannon M, Balla I, Ikrenyi C (2000) Physiological time series: distinguishing fractal noises from motions. *Eur J Physiol* 439:403–415
- Eke H, Herman P, Kocsis L, Kozak L (2002) Fractal characterization of complexity in temporal physiological signals. *Physiol Meas* 23:R1–R38
- Elliott D, Binsted G, Heath M (1999) The control of goal-directed limb movements: correcting errors in the trajectory. *Hum Mov Sci* 18:121–136
- Elliott D, Helsen WF, Chua R (2001) A century later: Woodworth's (1899) two-component model of goal-directed aiming. *Psychol Bull* 127:342–357
- Elliott D, Hansen S, Mendoza J, Tremblay L (2004) Learning to optimize speed, accuracy, and energy expenditure: a framework for understanding speed-accuracy relations in goal-directed aiming. *J Mot Behav* 3:339–351
- Farrell S, Wagenmakers EJ, Ratcliff R (2006) $1/f$ noise in human cognition: is it ubiquitous, and what does it mean? *Psychon Bull Rev* 4:737–741
- Gardner M (1978) Mathematical games: white and brown music, fractal curves and one-over-f fluctuations. *Sci Am* 238:16–32
- Glover S (2004) Separate visual representations in the planning and control of action. *Behav Brain Sci* 27:3–78
- Gordon J, Ghez C (1987) Trajectory control in targeted force impulses: III. Compensatory adjustments for initial errors. *Exp Brain Res* 2:253–269
- Hansen S, Glazebrook CM, Anson JG, Weeks DJ, Elliott D (2006) The influence of advance information about target location and visual feedback on movement planning and execution. *Can J Exp Psychol* 60:200–208
- Hansen S, Elliott D, Tremblay L (2007) Online control of discrete action following visual perturbation. *Perception* 36:268–287
- Hausdorff J, Purdon P, Peng C, Ladin Z, Wei J, Goldberger A (1996) Fractal dynamics in human gait: stability of long-range correlations in stride interval fluctuations. *J Appl Physiol* 80:1448–1457
- Holden J (2005) Gauging the fractal dimension of response times from cognitive tasks. In: Riley MA, Van Orden GC (eds) Contemporary nonlinear methods for behavioral scientists: a webbook tutorial, pp 267–318
- Keele SW (1968) Movement control in skilled motor performance. *Psychol Bull* 70:387–403
- Khan MA, Elliott D, Coull J, Chua R, Lyons J (2002) Optimal control strategies under different feedback schedules: kinematic evidence. *J Motor Behav* 34:45–47
- Killeen P (2005) Complex dynamic process in sign tracking with an omission contingency (negative automaintenance). *J Exp Psychol Anim Behav Process* 29:49–61
- Laming DRJ (1968) Information theory of choice-reaction times. Academic Press, London
- Laming DRJ (1979a) Autocorrelation of choice-reaction times. *Acta Psychol* 43:381–412
- Madison G (2001) Variability in isochronous tapping: higher order dependencies as a function of intertap interval. *J Exp Psychol Hum Percept Perform* 27:411–422
- Merrill WJ, Bennett CA (1956) The application of temporal correlation techniques in psychology. *J Appl Psychol* 40:272–280
- Messier J, Kalaska J (1999) Comparison of variability of initial kinematics and endpoints of reaching movements. *Exp Brain Res* 125:139–152
- Miyazaki M, Kadota H, Kudo K, Masani K, Ohtsuki T (2001) Fractal correlation of initial trajectory dynamics vanishes at the movement endpoint in human rapid goal-directed movements. *Neurosci Lett* 3:173–176
- Musha T, Katsurai K, Teramachi Y (1985) Fluctuations of human tapping intervals. *IEEE Trans Biomed Eng BME* 32:578–582
- Newell KM, Hoshizaki L, Carlton MJ (1979) Movement time and velocity as determinants of movement timing accuracy. *J Mot Behav* 1:49–58
- Ooms M, Doornik JA (1998, June) Estimation, simulation, and forecasting for fractional autoregressive integrated moving average models. Discussion paper, Econometric Institute, Erasmus University Rotterdam, presented at the fourth annual meeting of the Society for Computational Economics, Cambridge, UK
- Plamondon R, Alimi A (1997) Speed/accuracy trade-offs in target-directed movements. *Behav Brain Sci* 20:279–349

- Rangarajan G, Ding M (2000) Integrated approach to the assessment of long range correlation in time series data. *Phys Rev E* 61:4991–5001
- Scafetta N, Griffin L, West BJ (2003) Holder exponent spectra for human gait. *Physica A* 328:561–583
- Schmidt R, Lee T (2005) Motor control and learning: a behavioral emphasis. Human Kinetics, Champaign
- Smeets JBJ, Erkelens CJ, van der Gon JJ (1990) Adjustments of fast goal-directed movements in response to an unexpected inertial load. *Exp Brain Res* 81:303–312
- Taqqu MS, Teverosvsky V (1998) On estimating the intensity of long-range dependence in finite and infinite variance time series. In: Adler R, Feidman R, Taqqu MS (eds) *A practical guide to heavy tails: statistical techniques and applications*. Birkhauser, Boston, pp 177–217
- Thornton T, Gilden D (2005) Provenance of correlations in psychological data. *Psychon Bull Rev* 12:409–441
- Torre K, Delignieres D, Lemoine L (2007) Detection of long-range dependence and estimation of fractal exponents through ARFIMA modelling. *Br J Math Stat Psychol* 60:85–106
- Van Orden G, Holden J, Turvey M (2003) Self-organization of cognitive performance. *J Exp Psychol Gen* 132:331–350
- Verplanck W, Collier G, Cotton J (1952) Nonindependence of successive responses in measurements of the visual threshold. *J Exp Psychol* 44:273–281
- Wagenmakers E-J, Farrell S (2004) AIC model selection using Akaike weights. *Psychon Bull Rev* 11:192–196
- Wagenmakers E-J, Farrell S, Ratcliff R (2004) Estimation and interpretation of $1/f^{\alpha}$ noise in human cognition. *Psychon Bull Rev* 11:579–615
- Wagenmakers E-J, Farrell S, Ratcliff R (2005) Human cognition and a pile of sand: a discussion on serial correlation and self-organized criticality. *J Exp Psychol Gen* 132:108–116
- Weiss B, Coleman PD, Green RF (1955) A stochastic model for the time-ordered dependencies in continuous scale repetitive judgments. *J Exp Psychol* 50:237–244
- Wolpert DM, Gharamani Z (2000) Computational principles of movement neuroscience. *Nat Neurosci Suppl* 3:1212–1217
- Wolpert DM, Gharamani Z., Jordan M (1995) An internal model for sensorimotor integration. *Science* 269:1880–1882
- Woodworth RS (1899) The accuracy of voluntary movement. *Psychol Rev* 3(3, Suppl. 13):1–119
- Yamada M (1996) Temporal control mechanism in equaled interval tapping. *Appl Hum Sci* 15:105–110
- Yamada M, Yonera S (2001) Temporal control mechanism of repetitive tapping with simple rhythmic patterns. *Acoustical Sci Technol* 22:245–252